Metabolic Profiling in Mice Infected with Echinococcosis

Mingxing Zhu
Ningxia Medical University
Xiancai Du
Ningxia Medical University
Hongxia Xu
Ningxia Medical University
Songhao Yang
Ningxia Medical University
Chan Wang
Ningxia Medical University
Yazhou Zhu
Ningxia Medical University
Tingrui Zhang
Ningxia Medical University
wei zhao (weizhao@nxmu.edu.cn)
Ningxia Medical University https://orcid.org/0000-0002-7744-115X

Research

Keywords: Echinococcosis, metabolomics, metabolites, LC-MS/MS

Posted Date: February 4th, 2021

DOI: https://doi.org/10.21203/rs.3.rs-166281/v1

Abstract

Background: Echinococcosis is a severe zoonotic parasitic disease, which seriously affects the health of the hosts. The diagnosis of echinococcosis depends on objective detection of clinical symptoms. However, the patient is often in the late stage of the disease when the symptoms appear, limiting the early diagnosis of echinococcosis. The treatment and prognosis of the patients are seriously hampered due to long-term asymptomatic latency. Metabolomics is a new discipline developed in the late 1990s. It reflects a series of biological responses in a pathophysiological process by demonstrating the changes in metabolism under the influence of internal and external factors. When the organism is invaded by pathogens, the alteration in characteristics of metabolites in cells becomes exceedingly sensitive. Here, we used a liquid chromatography with tandem mass spectrometry (LC-MS/MS) system-based metabolomics approach to determine the molecular mechanism of cystic echinococcosis (CE) and to develop an effective method for CE diagnosis.

Methods: Eight-weeks-old female Balb/c mice were divided into normal and *Echinococcus granulosus* infection groups. To develop the *Echinococcus granulosus* infection model, mice were infected with protoscolex. Six weeks later, the abdomen of mice was obviously bulged. An LC-MS/MS system-based metabolomics approach was used for the analysis of the liver and feces to reveal the metabolic profiles of mice with echinococcosis.

Results: We found that the metabolism of nucleotides, alkaloids, amino acids, amides, and organic acids in mice is closely interrelated with *Echinococcus granulosus* infection

Conclusion: The metabolomics approach used in this study provides a reference for a highly sensitive and specific diagnostic and screening method for echinococcosis.

1. Background

Cystic echinococcosis (CE) or hydatidosis is a type of near-cosmopolitan zoonosis caused by *Echinococcus granulosus sensu lato* [1, 2]. The life cycle of *Echinococcus granulosus* involves two mammalian hosts. For the adult tapeworms, carnivores (canines and cats) are the definitive hosts, while ungulates and odontoids are intermediate hosts [3]. CE is prevalent in Western China, South America, Central Asia, Mediterranean, and East Africa [4]. The main risk factors are dogs and livestock [5–8]. Humans are not usually directly involved in the spread of CE. However, humans or intermediate hosts accidentally ingest eggs, which incubate in the intestines and release oncospheres [9]. The oncospheres are transported to the liver through the portal vein and lymphatic vessels where they settle and develop into larvae (hydatid cysts), rarely reaching the lungs, brains, bones or any other organ of a human or intermediate host [2, 10]. The growth of CE cysts is very slow [11]. There are no obvious symptoms in the early stage of CE, with more than half of cysts expressing no change in size in 10–15 years [12]. The clinical symptoms, such as epigastric discomfort or loss of appetite, commonly appear when the cyst becomes more than 10 cm long, and gradually develop causing damage and dysfunction in the parasitic

organs (mainly liver) [13, 14]. Clinically, the CE patients are in the late stage of echinococcosis when they present in the hospital. The cyst is frequently misdiagnosed as a tumor [15]. Therefore, determination of a positive and effective approach to discriminate CE patients from healthy people is conducive to the early diagnosis and treatment of echinococcosis, which can significantly improve the survival rate of patients.

Metabolomics, a new high-throughput sequencing technology introduced in recent years, is an important branch of omics and it has great potential in drug toxicity or safety evaluation [16]. Metabolomics reflects many factors, such as gene changes, nutritional status, pathogenesis, natural environment changes, drug treatment, physiological response, and pathological characteristics [17–21]. It is a dynamic observation of the occurrence and development of diseases and the transformation process [22]. In metabolomic studies, small molecule metabolites are used as the research object. It can be used to study drug metabolism, find differential metabolites, and explore the target and mechanism of action with the corresponding statistical analysis software using high sensitivity instruments (gas chromatography-mass spectrometry, nuclear magnetic resonance, liquid chromatography-mass spectrometry) [23–25]. Metabolomics has been widely used in a variety of hepatopathy to identify potential early biomarkers and metabolic pathways [26],which is a feasible measure to illustrate host-parasite interactions [27–29]. The metabolic state and biochemical activity of cells or tissues can be directly reflected by metabolites such as amino acids, lipids, or sugars [30, 31]. metabolic profiling approaches have been widely used in various studies on diseases caused by flatworms, *Fasciola hepatica* or *Onchocerca volvulus* [32–35]. Nevertheless, reports on the application of the LC-MS/MS-based metabolomics approach in echinococcosis is limited. In this study, we used a LC-MS/MS system-based metabolomics approach and multivariate statistical analyses to investigate the molecular mechanism of CE and to provide a potential valuable reference for the diagnosis of CE.

2. Methods

2.1 Establishment of hydatidosis model

Twenty 8-weeks-old female Balb/c mice, weighting about 18–22 g, were randomly divided into two groups: normal control group (n = 10) and *Echinococcus granulosus* infection group (n = 10). The mice were intraperitoneally injected with 2 ml PBS diluted protoscolex(containing 2000 protoscolex) to develop the *Echinococcus granulosus* infection model, The normal control group was intraperitoneally injected with the same 2 ml PBS. The liver and feces of both groups were obtained by dissection after 6 weeks of feeding. The mice models infected with *Echinococcus granulosus* were confirmed through routine pathological section staining.

The animal experiments were implemented in strict accordance with the laboratory animal management, with the approval from the Ningxia Medical University animal ethics committee and in accordance with the National Institute of Health guidelines for the Care and Use of Laboratory Animals.

2.2 Sample preparation

25mg liver and fecal Samples were weighed and transferred to a new clean EP tube. Add 500 μL extract solution (acetonitrile: methanol: water = 2:2:1) with isotopically labeled internal standard mixture to the sample. After 30 s of gentle vortex, the samples were homogenized at 35 Hz for 4 min and ultrasonicated in ice-water bath for 5 min. The procedure of homogenization and ultrasonication cycle was repeated three times. Then, the samples were incubated at -40°C for 1 hour and centrifuged at 4°C for 15 min at 12000 rpm. The ultimate resulting supernatant was transferred to a fresh and clean glass bottle for analysis. The quality control sample was prepared by mixing the supernatants of all samples of liver or feces in equal aliquot amounts.

2.3 LC-MS/MS analysis

LC-MS/MS analyses were performed by using a High performance liquid chromatography(HPLC) system (Vanquish, Thermo Fisher Scientific, Bruker Biospin, Karlsruhe, Germany). The injection volume of the liver and feces was 3 μL.

The MS/MS spectra were collected by QE HFX mass spectrometer in the control of the acquisition software (Xcalibur, Thermo). The acquisition software continuously evaluates the full scan MS spectrum in this mode. The conditions of ESI source were set as following: aux gas flow rate – 10 Arb, capillary temperature – 320°C,sheath gas flow rate – 50 Arb, full MS resolution – 60000, collision energy – 10/30/60 in NCE mode, MS/MS resolution – 7500, spray voltage – 3.5 kV (positive) or -3.2 kV (negative), respectively.

2.4 Metabolomics statistical analysis

The original data were converted to mzXML format by using ProteoWizard, and processed by an in-house program, which was based on XCMS and was developed using R. Metabolites were annotated using an in-house MS2 database (BiotreeDB). The cutoff value for annotation was set to 0.3.

2.5 Statistical analysis

SPSS software (version 20.0 for Windows) was used to analyzed the tata.and have been expressed as mean ± SD. In all cases, $P < 0.05$ was considered to be significant.

3. Results

3.1 Multivariate statistical analysis

In order to determine the metabolic changes in the liver and feces due to echinococcosis initiated following *Echinococcus granulosus* infection, two groups of samples were analyzed through principal component analysis (PCA). The metabolites of the liver were found to be moderate groupings between the infection and normal control groups under positive ion mode (POS) and negative ion mode (NEG) based on PCA (Fig. 1A and 1B). The interpretation rates of the first principal component (PC1) and second principal component (PC2) under POS were 33.5% and 17.6%, respectively, while under NEG, the respective interpretation rates were 30.9% and 15.6%. To better highlight the metabolic changes between

the two groups, Orthogonal Projections to Latent Structures-Discriminant Analysis (OPLS-DA) was performed. The difference between the two groups was evident in the OPLS-DA score plots (Fig. 1C and 1D). A similar tendency was observed in the metabolic changes in feces (fig. S1A, S1B, S1C, S1D). The group separation revealed that hydatid disease could cause obvious metabolic changes in the liver and feces of mice. All the samples were within the 95% confidence interval. In addition, the OPLS-DA models were supposed to be a good explanation for predictive powers Q^2 and variations R^2Y and with permutation tests (Fig. 1E, 1F, S1E, and S1F).

3.2 Screening of differential metabolites

In order to distinguish metabolic markers between the infection and control groups, the data are presented in the form of the volcano plots. The results of the metabolic changes were determined based on variable importance in the projection (VIP) > 1 and $P < 0.05$. The metabolites with enormous changes have been represented with blue or red dots and larger circle shapes, located in the upper left or right corner of the volcano plots. From the metabolites of the liver, 248 and 131 distinct metabolic molecules were screened under POS and NEG (Fig. 2A and 2B). In the feces, 201 and 58 various metabolites were screened under POS and NEG (fig. S2A and S2B). The top 15 metabolites with the most significantly different metabolism under POS and NEG in the liver and feces are shown in Table 1, Table 2, Table S1, and Table S2. In the livers of the infection group, the representative substances such as bile acid (deoxyviolaceinic acid), glycerides (2-O-(alpha-d-mannosyl)-d-glycerate), amino acids (glutaminylhistidine), and nucleotides (cytidine 2',3'-cyclic phosphate) were considerably upregulated, while nucleotides (inosinic acid and 5-fluorodeoxyuridine monophosphate) were remarkably downregulated under POS and in NEG. Furthermore, in the feces of the mice with echinococcosis, metabolites such as nucleotides (dTMP), alkaloids (piperine), amino acids (d-pantethine, d-aspartic acid, and gamma-glutamylleucine), and amides (N-acetylhistamine) were upregulated, while nucleosides (5'-methylthioadenosine), amino acids (3-methylcrotonylglycine, selenocystemic acid), organic acids (hexadecanedioic acid, dimethylmalonic acid, and ascorbic acid), and alkaloids (cytokinin b) were downregulated under POS and NEG (Table 1, 2, 3, and 4). The results suggest that the metabolism of nucleotides, alkaloids, amino acids, amides, and organic acids in mice is closely interrelated with *Echinococcus granulosus* infection.

3.3 Hierarchical clustering analysis of different metabolites

The discrepant metabolites by filtrating usually have similarity or complementarity of functions in biology, displaying similar or opposite expression characteristics among different experimental groups and the same metabolic pathway. The hierarchical clustering analysis of these characteristics of metabolites is helpful to classify the metabolites with the same characteristics into one category, as well as the variation characteristics of modern metabolites among the experimental groups.

For every sample, we calculated the Euclidean distance matrix to determine the quantitative value of the differential metabolites. The differential metabolites of the liver were clustered through the complete linkage method, and displayed in the thermodynamic diagram (Fig. 3A and 3B). Through further

evaluation, we selected 91 and 47 differential metabolic molecules under POS and NEG. Liver metabolites mainly included esters, amino acids, carbohydrates, and lipids. Compared with the normal control group, the expression of glyceric acid, acetylcysteine, myricetin, L-arabitol, L-asparagine, tryptophan, L-phenylalaine, racemethionine, D-alanine, D-proline, L-valine, and D-mannose were all increased in the infection group. Conversely, in the infection groups the levels of cholesterol sulfate, ribothymidine, ascorbic acid, alpha-linolenic acid, inosinic acid, adenine, thiamine, maltotetraose, creatinine, and imidazoleacetic acid were evidently decreased. Additionally, the levels of other metabolites were changed by various degrees. Fecal metabolic molecules were analyzed similarly; 107 and 23 differential molecules were selected under POS and NEG (fig. S3A and S3B). The expression of metabolic molecules such as medical acid, anandamide, piperine, N-carbamoyl putrescine, isoleucyl phenylalanine, D-aspartic acid, cytidine, and L-valine were sharply increased in the infection group. Besides, metabolic molecules such as trimethylaminoacetone, histidine, ophthalmic acid, hexadecanedioic acid, methylthioadenosine, traumatic acid, and phenylacetic acid showed a downward trend in the infection group. Coincidentally, L-valine was upregulated in the liver and feces in the infection group. The heat map (Fig. 3A and 3B) shows that the different metabolites had good classification results.

3.4 Correlation analysis of different metabolites

The complex metabolic reactions and their regulation do not occur in isolation after the mice are infected with *Echinococcus granulosus*. When different molecules work together, their interaction and regulation eventually lead to systematic changes in metabolomics. We calculated the correlation coefficient of the quantitative values of different metabolites and expressed it as r. In this study, 91 and 47 differential metabolic molecules in the liver under POS and NEG were analyzed through Pearson method. There was a clear correlation between amino acid metabolism (Fig. 4A and 4B). We also found that 107 and 23 differential molecules in the feces under POS and NEG were related (fig. S4A and S4B).

3.5 KEGG annotation of different metabolites

The analysis of the metabolic and regulatory pathways and systematic understanding of the changes in biological processes caused by changes in experimental conditions, pathogenesis of traits or diseases, and mechanism of drug action can be more comprehensive through KEGG annotation of different molecules. From the KEGG pathway map, we found that the differential metabolic molecules between the infection and control groups involved multiple pathways, including energy metabolism, material transport, signal transduction, and cell cycle regulation (Fig. 5A and 5B). In all, 46 pathways in the liver were involved with the differential metabolic molecules. In the feces, these differentially metabolized molecules involved 57 pathways (fig. S5A and S5B). For example, in the liver of the infected group, there were four differentially metabolized molecules that were enriched in purine metabolic pathways and three differentially metabolized molecules that were enriched in amino acid metabolic pathways. Similarly, in the feces of the infected group, three differential metabolic molecules were involved in pyrimidine metabolism, and two differential molecules were involved in arginine and proline metabolism. The more differential metabolic molecules involved in certain pathway, the more obvious the difference in the metabolic pathway between the infection and control groups.

3.6 Analysis of metabolic pathways of different metabolites

KEGG annotation analysis revealed all the pathways involved in the differential metabolites. In order to determine whether these metabolic pathways were closely related to the experimental conditions, it was necessary to further analyze the metabolic pathways of the differential metabolites. Through analysis by synthesis of the pathways (including topological analysis and enrichment analysis), we could further explore the pathways and find the key pathways with the highest correlation with metabolic differences. The results of metabolic pathway analysis were presented in bubble chart. In the liver, there were seven metabolic pathways under POS and NEG, three of which were in common. The metabolic pathways of tyrosine and tryptophan biosynthesis, phenylalanine, valine, leucine and isoleucine biosynthesis and phenylalanine metabolism were notably associated with the occurrence and development of hydatid disease (Fig. 6A and 6B). However, there were 15 metabolic pathways under POS and NEG, one of which is in common (fig.S6A and S6B), which revealed that pantothenate and CoA biosynthesis is also considerably related with echinococcosis.

4. Discussion

In this study, we analyzed the metabolic footprint and significant changes in metabolism, which revealed the substantial changes in the mice metabolome due to CE with the multivariate statistical analysis of liver and feces. In all, 138 metabolic molecules were selected to discriminate CE mice from healthy mice. Seven metabolic pathways appeared under POS and NEG, which can be considered to be related with echinococcosis. The three common metabolic pathways were tyrosine and tryptophan biosynthesis, phenylalanine, valine, leucine and isoleucine biosynthesis and phenylalanine metabolism, which indicated that amino acid metabolism is considerably associated with the occurrence and development of hydatid disease. These metabolic differences may provide a novel viewpoint into the biological mechanisms that occur during CE infection. Interestingly, 130 metabolic molecules in feces were considered to distinguish between the infection and control groups. These molecules were enriched in 15 pathways, one of which is in common under POS and NEG. The pantothenate and CoA biosynthesis pathway indicated that the metabolism of fatty acid and pyruvate in mice with echinococcosis would be disturbed.

The main organ involved in echinococcosis is the liver. With the cyst parasitization and growth, it continuously obtains nutrition from the liver. When it grows large enough, it oppresses the liver to change its structure and function [1, 36]. The results revealed that CE can lead to significant changes in amino acid metabolism. The level of circulating of amino acids indicate the equilibrium between muscle and liver metabolism [37].

It was confirmed by increased phenylalanine and tyrosine levels in the infection group. Tyrosine is the foremost product of Phenylalanine. It has been reported that the concentrations of these two metabolites are the same. The conversion of phenylalanine to tyrosine occurs uniquely in the liver [38, 39]. The catabolism of amino acids occurs mainly in the liver [40]. Liver injury can lead to changes in amino acid

metabolism, mainly manifested as the decrease in free branched chain amino acids and increase in free amino acids (phenylalanine, tryptophan and tyrosine) [41]. In contrast with the normal mice, the molecular metabolites of the liver and feces were related in infected mice. Among the first 15 most differentially metabolized molecules, tolclofos methyl was increased in the liver and reduced in the feces, chlorfenson was downregulated in the liver and upregulated in the feces while aminosalicylate sodium anhydrous and Disul were both decreased in the liver and feces. In conclusion, the reason why amino acids (phenylalanine, tyrosine, tryptophan, valine, leucine, and isoleucine) were increased in the infection group may be related to liver dysfunction. We noticed that purine metabolism and alpha-linolenic acid metabolism were abnormal in CE mice, which suggests that other pathways may participate in the metabolism after hydatid infection as well.

The limitations of this study were as follows. First, the current results need more samples to verify and further improve its reliability and accuracy. Secondly, the comprehensive application of LC-MS with GC-MS or NMR will expand the coverage of metabolomics. Moreover, a variety of omics technologies (such as genomics and proteomics) can be cross-validated and may better support the experimental results. Finally, no effective method was determined to distinguish echinococcosis from other types of liver disease in this study. If the method is developed, it is essential to prevent clinical misdiagnosis because echinococcosis is similar to other hepatic diseases. The feasibility of using Fischer ratio and unique metabolic characteristics of echinococcosis to identify different liver diseases warrants further study.

The LC-MS method is suitable for metabolomics of hydatid disease due to its repeatability, multiple metabolite coverage in one measurement and short detection duration. The systematic research of multiple metabolites of small molecules is helpful in revealing the overall metabolic changes induced by *Echinococcus granulosus*. The early diagnosis of echinococcosis may be feasible by combining both imaging techniques and metabolomics. For example, chemical-exchange weighted magnetic resonance imaging techniques are used to yield maps weighted by metabolites of interest [42–44]. These maps are obtained by exchange with water and are characterized by significant enhancement of the signal and the observation of small metabolic changes that cannot be noticed by other imaging methods. Unfortunately, the common problem with these technologies is the lack of specificity. LC-MS-based metabolomics with specificity can be combined to enhance the analysis and better explain the data.

5. Conclusion

In our study, LC-MS-based metabolomics was used for investigating metabolic diversification of CE. It was confirmed that amino acid metabolism (phenylalanine, tyrosine, tryptophan, valine, leucine, and isoleucine) and pantothenate and CoA biosynthesis changed significantly in hydatid infection. The particular metabolic changes found in this study may provide new understanding of the molecular mechanism of CE and provide some meaningful clues for the early diagnosis and therapeutic intervention of CE.

Abbreviations

LC-MS/MS
Liquid chromatography with tandem mass spectroscopy
CE
Cystic echinococcosis
PCA
Principal Component Analysis
POS
Positive ion mode
NEG
Negative ion mode
IDA
Information-dependent acquisition
OPLS-DA
Orthogonal Projections to Latent Structures-Discriminant Analysis

Declarations

Authors' contributions

XCD, MXZ, HXX and WZ designed the experiment together. CW and SHY made echinococcosis model in mice. TRZ and YZZ gathered the data. XXD finished the manuscript. MXZ and HXX provided financial support for the project. All authors read and approved the final manuscript.

Funding

This work was supported by the grants from the National Natural Science Foundation of China (No.81560335, No.32060805), the Natural Scence Foundation of Ningxia Hui Autonomous Region (2019AAC03264, 2018AAC03208), and the Foundation of Ningxia Medical University (XT2019020).

Availability of data and materials

The data of the results of this study are included in this paper and its attached files.

Ethics approval and consent to participate

All the experiments were approved by the ethics committee of Ningxia Medical University and complied with the guidelines of all institutions and countries on experimental animals. The data obtained met the appropriate ethical requirements.

Consent for publication

Not applicable.

Competing interests

The author states that they have no competing interests.

Acknowledgements

The authors would like to thank the Center of Scientific Technology of Ningxia Medical University for sharing the instruments.

References

1. Mcmanus DP, Gray DJ, Zhang W, Yang Y. Diagnosis, treatment, and management of echinococcosis. BMJ. 2012;344:e3866.
2. Larrieu E, Gavidia CM, Lightowlers MW. Control of cystic echinococcosis: Background and prospects. Zoonoses Public Health. 2019;66(8):889–99.
3. Mcmanus DP, Zhang W, Li J, Bartley PB. Echinococcosis Lancet. 2003;362(9392):1295–304.
4. Romig T. Epidemiology of echinococcosis. Langenbecks Arch Surg. 2003;388(4):209–17.
5. Deplazes P, Rinaldi L, Alvarez Rojas CA, Torgerson PR, Harandi MF, Romig T, et al. Global distribution of alveolar and cystic echinococcosis. Adv Parasitol. 2017;95:315–493.
6. Larrieu E, Zanini F. Critical analysis of cystic echinococcosis control programs and praziquantel use in South America, 1974–2010. Rev Panam Salud Publ = Pan. Am J Public Health. 2012;31(1):81–7.
7. Craig PS, Hegglin D, Lightowlers MW, Torgerson PR, Wang Q. Echinococcosis: Control and prevention. Adv Parasitol. 2017;96:55–158.
8. Tünger Ö. [Epidemiology of cystic echinococcosis in the world].[J]. Turk Parazitolojii Derg. 2013;37(1):47–52.
9. Casulli A, Siles-Lucas M, Tamarozzi F. Echinococcus granulosus sensu lato. Trends Parasitol. 2019;35(8):663–4.
10. Wen H, Vuitton L, Tuxun T, Li J, Vuitton DA, Zhang W, et al. Echinococcosis: Advances in the 21st Century. Clin Microbiol Rev. 2019;32(2):e18–75.
11. Kern P, Menezes Da Silva A, Akhan O, Müllhaupt B, Vizcaychipi KA, Budke C, et al. The echinococcoses: Diagnosis, clinical management and burden of disease. Adv Parasitol. 2017;96:259–369.
12. Romig T, Dinkel A, Mackenstedt U. The present situation of echinococcosis in Europe. Parasitol Int. 2006;55;Suppl:S187–91.
13. Frider B, Larrieu E, Odriozola M. Long-term outcome of asymptomatic liver hydatidosis. J Hepatol. 1999;30(2):228–31.
14. Agudelo Higuita NI, Brunetti E, Mccloskey C. Cystic echinococcosis. J Clin Microbiol. 2016;54(3):518–23.
15. Tao S, Qin Z, Hao W, Yongquan L, Lanhui Y, Lei Y. Usefulness of gray-scale contrast-enhanced ultrasonography (SonoVue®) in diagnosing hepatic alveolar echinococcosis. Ultrasound Med Biol.

2011;37(7):1024–8.
16. Bujak R, Struck-Lewicka W, Markuszewski MJ, Kaliszan R. Metabolomics for laboratory diagnostics. J Pharm Biomed Anal. 2015;113:108–20.
17. Laíns I, Gantner M, Murinello S, Lasky-Su JA, Miller JW, Friedlander M, et al. Metabolomics in the study of retinal health and disease. Prog Retin Eye Res. 2019;69:57–79.
18. Jang C, Chen L, Rabinowitz JD. Metabolomics and isotope tracing. Cell. 2018;173(4):822–37.
19. Chen X, Yu D. Metabolomics study of oral cancers. Metabolomics. 2019;15(2):22.
20. Filla LA, Edwards JL. Metabolomics in diabetic complications. Mol Biosyst. 2016;12(4):1090–105.
21. Ghatak A, Chaturvedi P, Weckwerth W. Metabolomics in plant stress physiology. Adv Biochem Eng/biotechnology. 2018;164:187–236.
22. Nicholson JK, Lindon JC, Holmes E. “Metabonomics”: Understanding the metabolic responses of living systems to pathophysiological stimuli via multivariate statistical analysis of biological NMR spectroscopic data[J]. null. Xenobiotica. 1999;29(11):1181–9.
23. Uehara T, Horinouchi A, Morikawa Y, Tonomura Y, Minami K, Ono A, et al. Identification of metabolomic biomarkers for drug-induced acute kidney injury in rats. J Appl Toxicol. 2014;34(10):1087–95.
24. Wang P, Shehu AI, Ma X. The opportunities of metabolomics in drug safety evaluation. Curr Pharmacol Rep. 2017;3(1):10–5.
25. Griffin JL. Twenty years of metabonomics: So what has metabonomics done for toxicology? Xenobiotica. 2020;50(1):110–4.
26. Amathieu R, Triba MN, Goossens C, Bouchemal N, Nahon P, Savarin P, et al. Nuclear magnetic resonance based metabolomics and liver diseases: Recent advances and future clinical applications. World J Gastroenterol. 2016;22(1):417–26.
27. Nicholson JK, Holmes E, Kinross JM, Darzi AW, Takats Z, Lindon JC. Metabolic phenotyping in clinical and surgical environments. Nature. 2012;491(7424):384–92.
28. SenGupta A, Ghosh S, Das BK, Panda A, Tripathy R, Pied S, et al. hosts Mol Biosyst. 2016;12(11):3324–32.
29. Wang Y, Li JV, Saric J, Keiser J, Wu J, Utzinger J, et al. Advances in metabolic profiling of experimental nematode and trematode infections. Adv Parasitol. 2010;73:373–404.
30. Fernie AR. The future of metabolic phytochemistry: Larger numbers of metabolites, higher resolution, greater understanding. Phytochemistry. 2007;68(22–24):2861–80.
31. Reaves ML, Rabinowitz JD. Metabolomics in systems microbiology. Curr Opin Biotechnol. 2011;22(1):17–25.
32. Saric J, Li JV, Wang Y, Keiser J, Veselkov K, Dirnhofer S, et al. Panorganismal metabolic response modeling of an experimental Echinostoma caproni infection in the mouse. J Proteome Res. 2009;8(8):3899–911.

33. Saric J, Li JV, Wang Y, Keiser J, Bundy JG, Holmes E, et al. Metabolic profiling of an Echinostoma caproni infection in the mouse for biomarker discovery. PLOS Negl Trop Dis. 2008;2(7):e254.
34. Saric J, Li JV, Utzinger J, Wang VL, Keiser J, Dirnhofer S, et al. Systems parasitology: Effects of Fasciola hepatica on the neurochemical profile in the rat brain.[Z]. 2010;6:396.
35. Denery JR, Nunes AAK, Hixon MS, Dickerson TJ, Janda KD. Metabolomics-based discovery of diagnostic biomarkers for onchocerciasis. PLOS Negl Trop Dis. 2010;4(10).
36. Eckert J, Deplazes P. Biological, epidemiological, and clinical aspects of echinococcosis, a zoonosis of increasing concern. Clin Microbiol Rev. 2004;17(1):107–35.
37. Tietge UJF, Bahr MJ, Manns MP, Böker KH. Hepatic amino-acid metabolism in liver cirrhosis and in the long-term course after liver transplantation. Transpl Int. 2003;16(1):1–8.
38. Dejong CHC, van de Poll MCG, Soeters PB, Jalan R, Olde D, steven WM. Aromatic amino acid metabolism during liver failure. J Nutr. 1597s-1598S;2007:137(6 Suppl 1): 1579S-1585S.
39. Abu-Omar MM, Loaiza A, Hontzeas N. Reaction mechanisms of mononuclear non-heme iron oxygenases. Chem Rev. 2005;105(6):2227–52.
40. Genchi G. An overview on D-amino acids. Amino Acids. 2017;49(9):1521–33.
41. Mcallan L, Cotter PD, Roche HM, Korpela R, Nilaweera KN. Impact of leucine on energy balance. J Physiol Biochem. 2013;69(1):155–63.
42. Cai K, Haris M, Singh A, Kogan F, Greenberg JH, Hariharan H, et al. Magnetic resonance imaging of glutamate. Nat Med. 2012;18(2):302–6.
43. Zhou J, Tryggestad E, Wen Z, Lal B, Zhou T, Grossman R, et al. Differentiation between glioma and radiation necrosis using molecular magnetic resonance imaging of endogenous proteins and peptides. Nat Med. 2011;17(1):130–4.
44. van Zijl PCM, Lam WW, Xu J, Knutsson L, Stanisz GJ. Magnetization Transfer Contrast and Chemical Exchange Saturation Transfer MRI. Features and analysis of the field-dependent saturation spectrum. NeuroImage. 2018;168:222–41.

Tables

Due to technical limitations, table 1 & 2 is only available as a download in the Supplemental Files section.

Supplementary Information

S1. PCA (A and B), OPLS-DA (C and D) score plots and OPLS-DA permutation plots (E and F) in feces A and B. PCA score plots, the abscissa PC1 and the ordinate PC2 represent the scores of the principal components ranking the first and the second, respectively, and different shapes of the scattered points represent the different groups of the samples. C and D. OPLS-DA score plots, the ordinate t[1]O represents the orthogonal principal component score, the abscissat[1]P represents the predicted principal component score of the first principal component, and different shapes of the scattered points represent the different groups of the samples. E and F. OPLS-DA permutation plots. The abscissa correlation

coefficient represents relevance. The Q2 and R2Y values reflect the model predictability and the fraction of explained variance, respectively. S2. volcano plots in feces (A and B) A and B. volcano plots, each dot in the volcano map represents a metabolite, the abscissa shows the Fold change value (take the logarithm of cardinal number 2), the ordinate represents the P-value of student's t-test (take the negative number of base logarithm of 10), and the size of the scatter represents the VIP value of OPLS -DA model, the larger the scatter, the greater the VIP value. S3. heat map in feces (A and B) A and B. The abscissa indicates different experimental groups, the ordinate means different metabolites compared with the normal control group, and the square color blocks at different spaces represent the relative expression of metabolites at corresponding positions. S4. Heat map of correlation analysis for group in feces (A and B) A and B. The abscissa and ordinate represent the different metabolites of the group comparison. The square color pathes in different positions represent the correlation coefficient between the two metabolites at corresponding positions. Red shows positive correlation, blue shows negative correlation, and the darker the color, the stronger the correlation. At the same time, the nonsignificant correlation was marked with a cross. S5. KEGG pathways map in feces (A and B) A and B. KEGG pathways map, the red and blue dots indicate the metabolic pathways involved by the differentially expressed metabolites. S6. Pathway analysis for group in feces (A and B) A and B. Pathway analysis for group, In the bubble plots, different bubbles represent different metabolic pathway. The abscissa and the size of bubble indicate the influence factor of the pathway in topological analysis. The larger the size is, the greater the influence factors are. The ordinate and the color of the bubble show the p value of enrichment analysis (negative natural pair, i.e. - in (P)). The deeper the color, the smaller the p value, the more significant the enrichment degree.

Figures

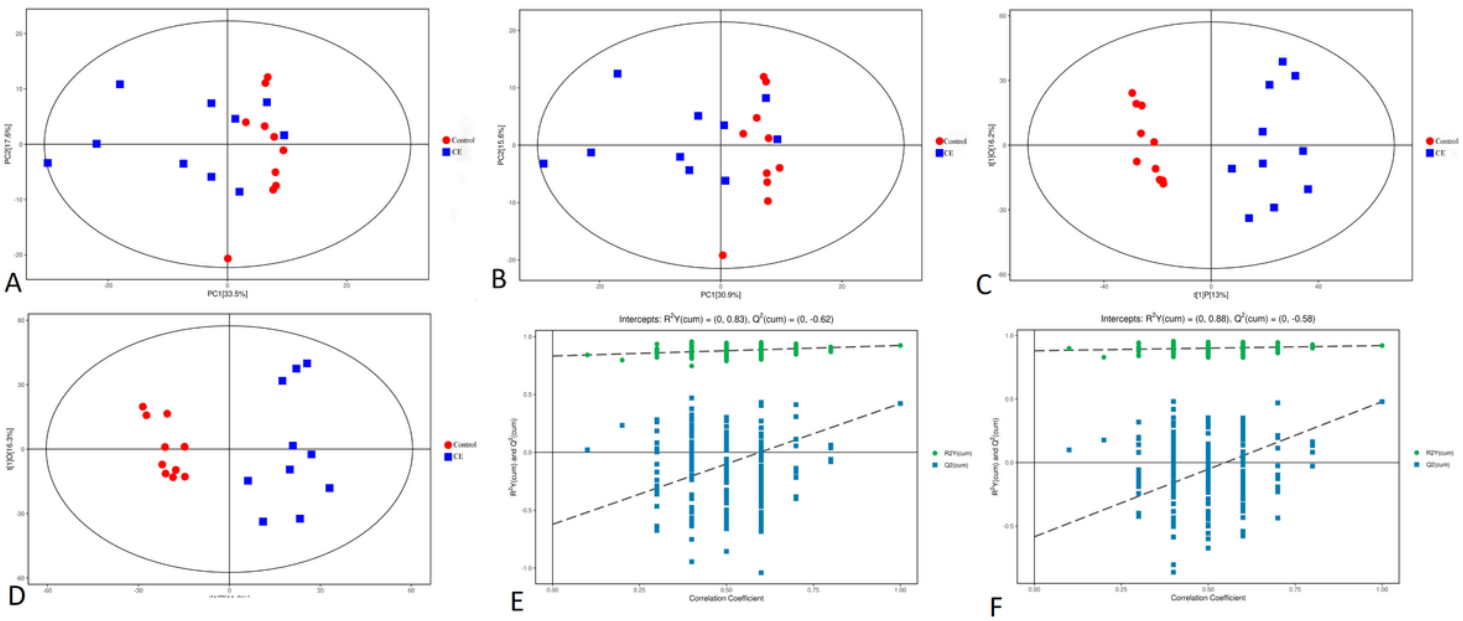

Figure 1

PCA (A and B), OPLS-DA (C and D) score plots and OPLS-DA permutation plots (E and F) in liver A and B. PCA score plots, the abscissa PC1 and the ordinate PC2 represent the scores of the principal components ranking the first and the second, respectively, and different shapes of the scattered points represent the different groups of the samples. C and D. OPLS-DA score plots, the ordinate t[1]O represents the orthogonal principal component score, the abscissat[1]P represents the predicted principal component score of the first principal component, and different shapes of the scattered points represent the different groups of the samples. E and F. OPLS-DA permutation plots. The abscissa correlation coefficient represents relevance. The Q2 and R2Y values reflect the model predictability and the fraction of explained variance, respectively.

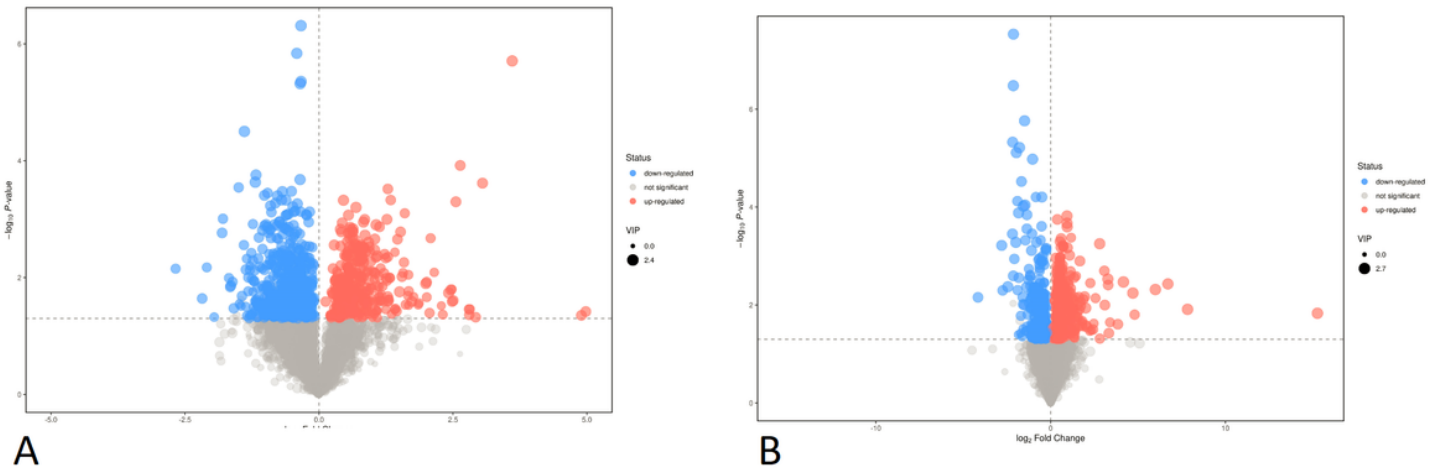

Figure 2

volcano plots in liver (A and B) A and B. volcano plots, each dot in the volcano map represents a metabolite, the abscissa shows the Fold change value (take the logarithm of cardinal number 2) , the ordinate represents the P-value of student's t-test (take the negative number of base logarithm of 10), and the size of the scatter represents the VIP value of OPLS -DA model, the larger the scatter, the greater the VIP value.

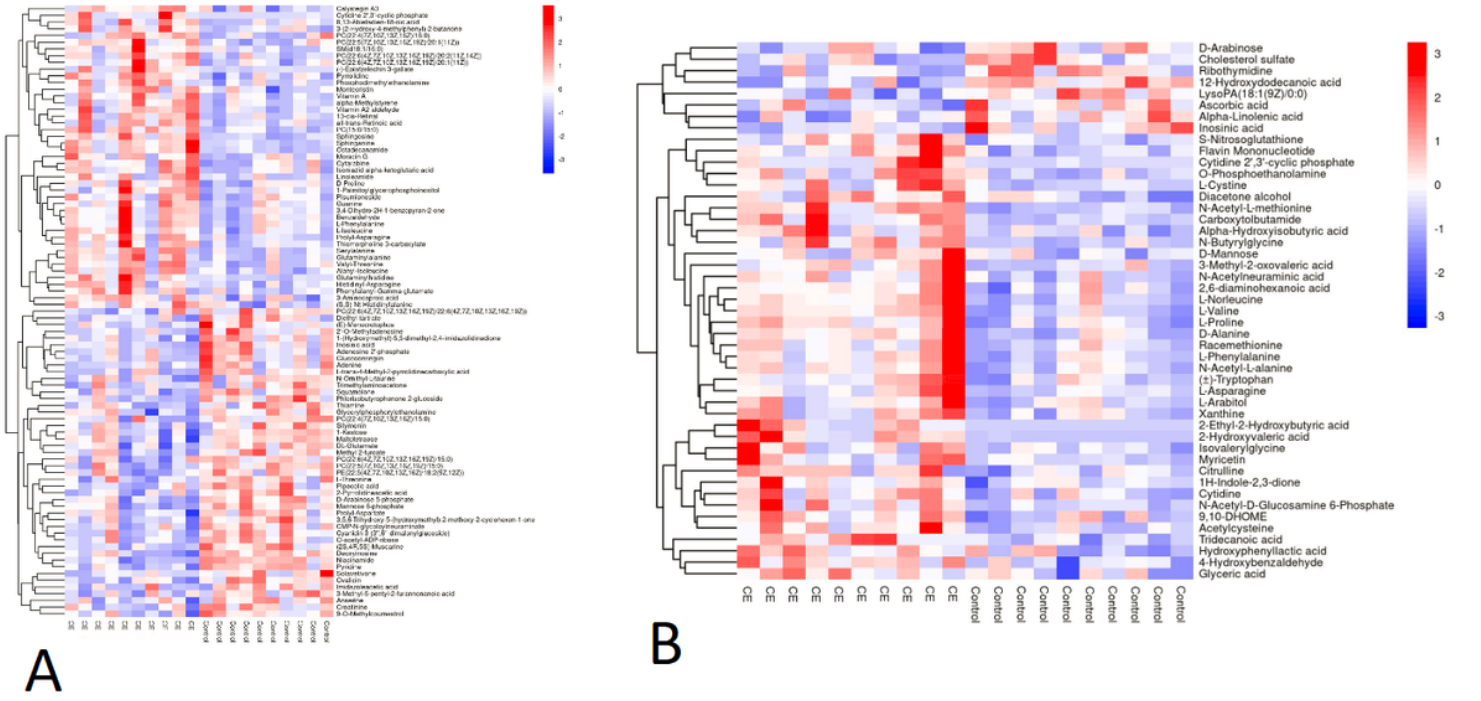

Figure 3

heat map in liver (A and B) A and B. The abscissa indicates different experimental groups, the ordinate means different metabolites compared with the normal control group, and the square color blocks at different spaces represent the relative expression of metabolites at corresponding positions.

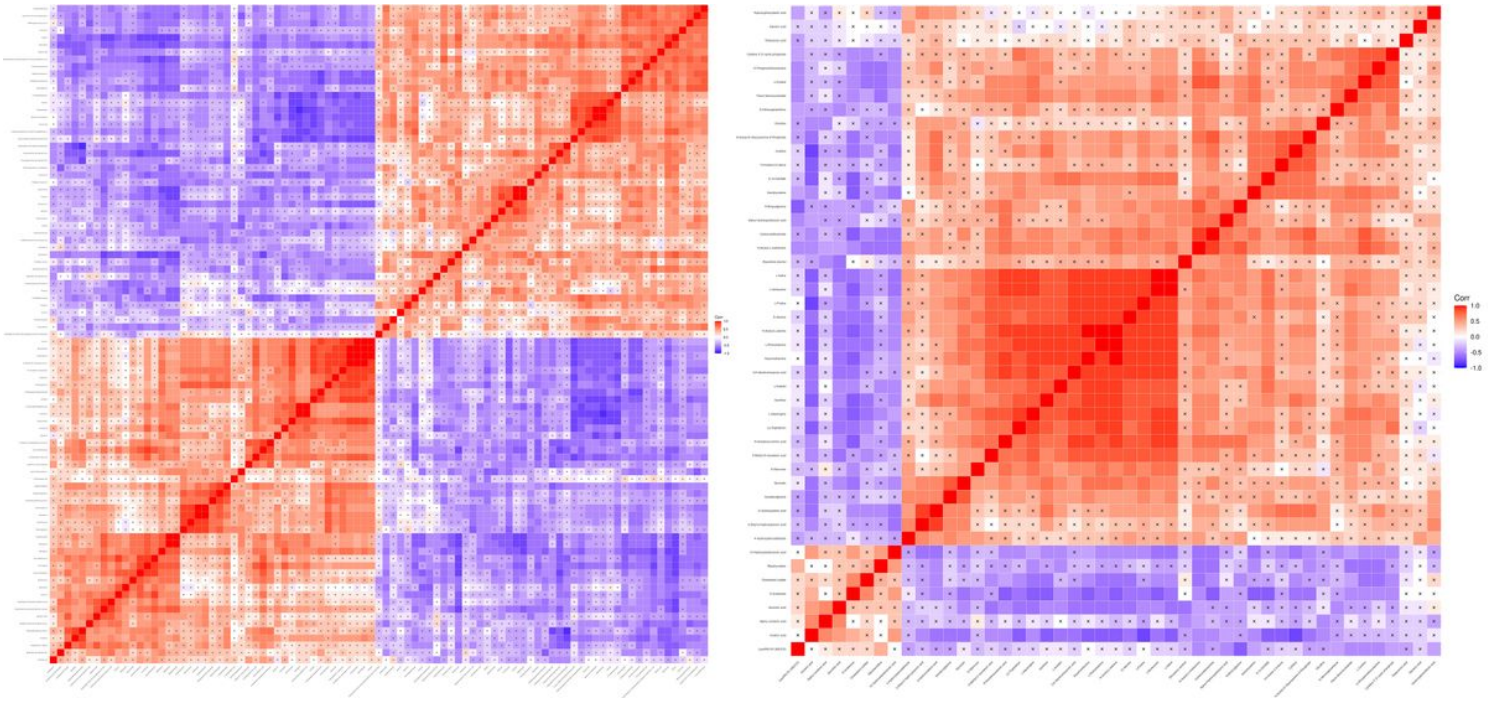

Figure 4

Heatmap of correlation analysis for group in liver (A and B) A and B. The abscissa and ordinate represent the different metabolites of the group comparison. The square color pathes in different positions

represent the correlation coefficient between the two metabolites at corresponding positions. Red shows positive correlation, blue shows negative correlation, and the darker the color, the stronger the correlation. At the same time, the nonsignificant correlation was marked with a cross.

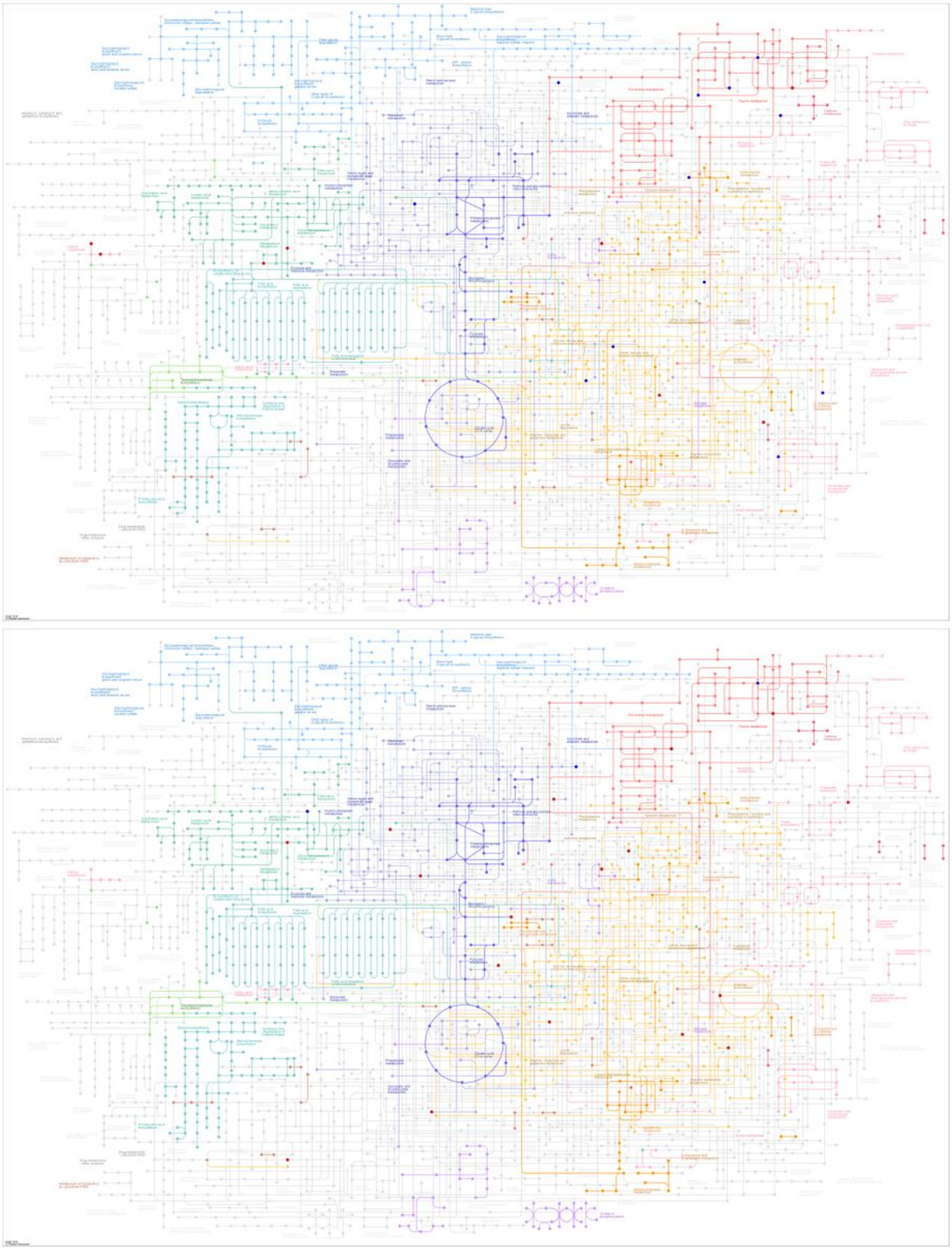

Figure 5

KEGG pathways map in liver (A and B) A and B. KEGG pathways map, the red and blue dots indicate the metabolic pathways involved by the differentially expressed metabolites.

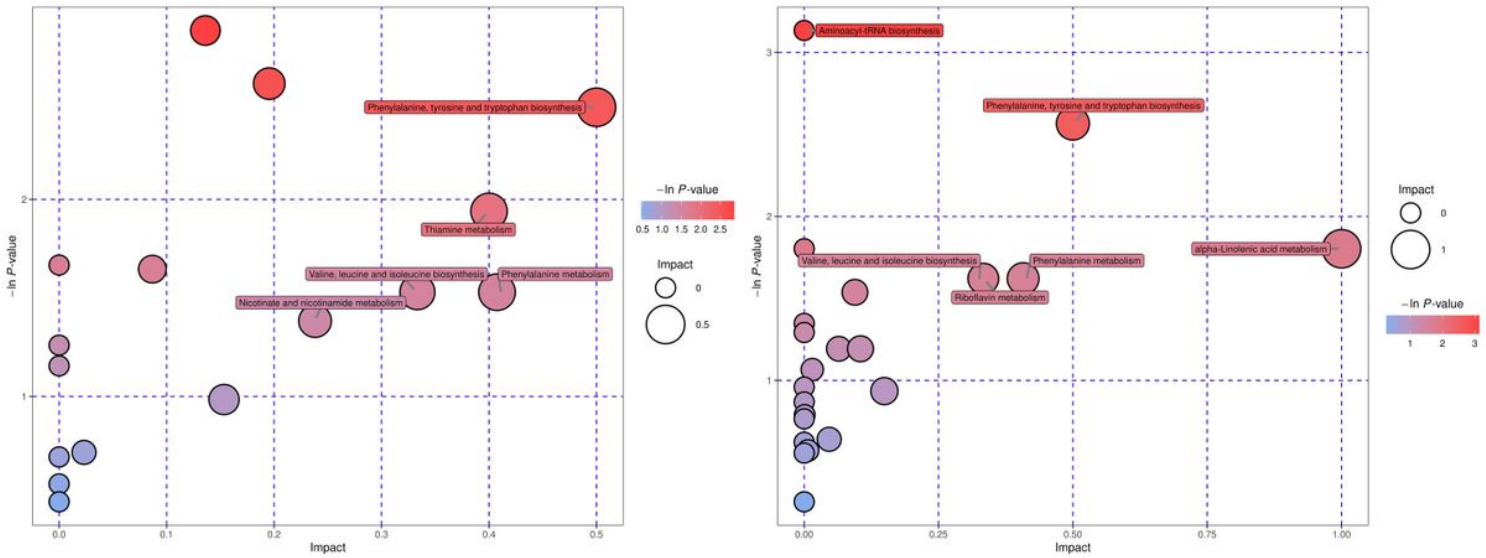

Figure 6

Pathway analysis for group in liver (A and B) A and B. Pathway analysis for group, In the bubble plots, different bubbles represent different metabolic pathway. The abscissa and the size of bubble indicate the influence factor of the pathway in topological analysis. The larger the size is, the greater the influence factors are. The ordinate and the color of the bubble show the p value of enrichment analysis (negative natural pair, i.e. - in (P)). The deeper the color, the smaller the p value , the more significant the enrichment degree.

Supplementary Files

This is a list of supplementary files associated with this preprint. Click to download.

- Table1.png
- Table2.png
- GraphicalAbstract.jpg
- Sfig1APOSPCAscoreplot.tif
- Sfig1BNEGPCAscoreplot.tif
- Sfig1CPOSOPLSDAscoreplot.tif
- Sfig1DNEGOPLSDAscoreplot.tif
- Sfig1EPOSOPLSDApermutationplot.jpg
- Sfig1FNEGOPLSDApermutationplot.jpg
- S2Avolcanoplot.jpg
- S2Bvolcanoplot.jpg
- Sfig3Aheatmap.jpg
- Sfig3Bheatmap.jpg

- Sfig4Aheatmap.tif
- Sfig4BCorrelationplot.jpg
- Sfig5Ammu01100.png
- Sfig5Bmmu01100.png
- Sfig6ABubblePlot.jpg
- Sfig6BBubblePlot.jpg
- TableS1.png
- TableS2.png